Nicotiana benthamiana protein, NbPCIP1, interacting with Potato virus X coat protein plays a role as susceptible factor for viral infection

Mi-Ri Park, Sang-Ho Park, Sang-Yun Cho, Kook-Hyung Kim *

Department of Agricultural Biotechnology and Plant Genomics and Breeding Institute, Seoul National University, Seoul 151-921, Republic of Korea

A B S T R A C T

The interactions of viral coat protein (CP) and host factors play an important role in viral replication and/or host defense mechanism. In this study, we constructed Nicotiana benthamiana cDNA library to find host factors interacting with Potato virus X (PVX) CP. Using yeast two-hybrid assay, we screened 3.3×10^6 independent yeast transformants from N. benthamiana cDNA library and identified six positive clones. One positive clone, named PVX CP-interacting protein 1 (NbPCIP1), is a plant-specific protein with homologue in N. tabacum (GenBank accession no. AB04049). We confirmed the PVX CP–NbPCIP1 interaction using yeast-two hybrid assay in yeast, protein–protein binding assay in vitro, and bimolecular fluorescent complementation assay in planta. Quantitative real-time RT-PCR analysis showed that the mRNA level of NbPCIP1 increased in PVX-infected N. benthamiana plants as compared to that of healthy plants. The green fluorescent protein (sGFP)-fused NbPCIP1 (NbPCIP1-sGFP) was localized in ER or ER-associated granular-like structure of cells. When we co-express NbPCIP1-sGFP and red fluorescent protein (RFP)-fused PVX CP (PVX CP-RFP), which were introduced by transiently expressing these proteins in N. benthamiana protoplasts and epidermal cells, however, we observed the co-localization of these proteins in the inclusion body-like complex in areas surrounding nucleus. Transient over-expression and transgene silencing of NbPCIP1 assay analysis indicated that NbPCIP1 plays a critical role in viral replication during PVX infection in host plant.

© 2009 Elsevier Inc. All rights reserved.

Introduction

The infection of susceptible plants by RNA viruses requires compatible interactions between host and viral factors and thus host factors play an essential role in virus infection. In general, viral and host factors modulate RNA virus replication processes by stabilizing RNA–RNA, RNA–protein, and protein–protein interactions in many steps during plant virus replication (Diez et al., 2000; Gamarnik and Andino, 1998; Huisman et al., 1988; Ishikawa et al., 1997; Strauss and Strauss, 1999). Coat protein (CP), encoded by several plus-strand plant RNA viruses, are first exposed to the surrounding environment during their initial infection step (Callaway et al., 2001) and thus one of the first candidates interacting with host factors. CP plays a major role in symptom development, viral RNA replication, systemic movement, cell-to-cell movement, and cross-protection in many RNA plant viruses (Callaway et al., 2001; Carrington et al., 1996; Lazarowitz and Beachy, 1999; Lu et al., 1998) and these diverse abilities of CP suggest that CP may be involved in suppression or evasion of some plant defense response by interacting with host factors (Callaway et al., 2001; Okinaka et al., 2003).

A limited number of host proteins have been demonstrated to interact with CPs of plant RNA viruses (Hofius et al., 2007; Krab et al., 2005; Li et al., 2005; Okinaka et al., 2003). For example, it has been reported that the CP of Alfalfa mosaic virus (AMV), a member of the genus Alfamovirus, specifically interacts with eIF4G and eIFiso4G and stimulate translation of the viral RNAs (Krab et al., 2005). Recently, the specific interaction of Potato virus Y (PVY) CP with DnaJ-like proteins from Nicotiana tabacum and its possible role in CP-mediated recruitment of host HSP70-related chaperones for PVY pathogenesis were also reported (Hofius et al., 2007). Although we have known that some plant RNA viral CP play an important role(s) in host–viral protein interactions for virus replication in host plants as described in PVY and AMV systems, the host protein(s) that interact with CPs of most of the other plant RNA viruses including Potato virus X (PVX) are largely unknown.

PVX, the type member of the genus Potexvirus, is a flexuous rod shape virus containing a 6.4 kb plus-strand RNA genome (Bercks, 1970). The PVX genome, which is capped and polyadenylated, consists of an 84 nucleotide (nt) at the 5′ non-translated region (NTR), five open reading frames (ORFs), and a 72 nt at 3′ NTR (Bercks, 1970; Huisman et al., 1988; Skryabin et al., 1988). The 5′ NTR contains AC-rich sequences and several repeat ACCA motifs followed by at least one stable stem–loop, SL1 which are all important for PVX RNA replication (Kim and Hemenway, 1996; Miller et al., 1998, 1999; Park et al., 2008a, 2008b). It has also been demonstrated that the unknown host factor (p54) as well as CP-binding elements are also located within AC-rich sequence and SL1

* Corresponding author. Fax: +82 2 873 2317.
  E-mail address: kookkim@snu.ac.kr (K.-H. Kim).

structure at the 5′ region and that the binding of CP subunits to the SL1 structure was sufficient for the formation of virus like particles (Kim et al., 2002; Kwon et al., 2005). Recently, it was further confirmed that the 5′-terminal region of PVX RNA was encapsidated selectively in single-tailed RNA-CP particles and modulates the nature of the infectious virus transport form through the binding with TGBp1 (Karpova et al., 2006) and also acts as a *cis*-acting element essential for cell-to-cell movement of RNA (Lough et al., 2006). In addition, the importance of sequences and structures in the PVX 3′ NTR for accumulation of viral RNAs has also been reported (Hu et al., 2007; Pillai-Nair et al., 2003). ORF1 encodes the viral replicase (165 kDa), which is the only viral protein absolutely required for PVX RNA synthesis. The function of viral cell-to-cell movement is associated with the triple gene block (TGB), ORFs 2–4 (Agros et al., 1980; Bercks, 1970). The PVX TGB ORFs are partly overlapping and encode the 25, 12, and 8 kDa proteins. ORF5 encodes viral CP, which is required for encapsidation and viral cell-to-cell movement (Chapman et al., 1992; Oparka et al., 1996).

Nicotiana benthamiana is the most widely used experimental host plant in plant virology because most plant viruses can successfully infect it. Additionally, *N. benthamiana* is rapidly gaining popularity in plant biology, particularly in studies requiring protein localization, interaction, or plant-based systems for protein expression and purification because it can be genetically transformed and regenerated with good efficiency and is easily applicable for characterizing gene functions by virus-induced gene silencing (VIGS) or transient over-expression of specific proteins (Goodin et al., 2008). To identify host factors that interact with PVX CP, we constructed an *N. benthamiana* cDNA library and screened cDNA library using yeast-two hybrid assay. We identified a host protein, named *N. benthamiana* *P*VX *C*P-*I*nteracting *P*rotein 1 (NbPCIP1), interacting with PVX CP. We show that NbPCIP1 interacts with PVX CP in yeast, *in vitro*, and *in planta* by yeast-two hybrid assay, *in vitro* binding assay, and bimolecular fluorescent complementation (BiFC) assay, respectively. We observed that NbPCIP1 was localized in endoplasmic reticulum (ER) and that the sGFP-fused NbPCIP1 in the presence of PVX CP was co-localized in inclusion body-like complex in areas surrounding the nucleus in *N. benthamiana* protoplasts and plants. Transient over-expression and transgene silencing of NbPCIP1 by agro-infiltration

suggest that NbPCIP1 positively affect PVX replication and movement in *N. benthamiana* plants.

Results

Isolation of NbPCIPs, PVX CP-interacting proteins

To identify host proteins interacting with PVX CP, a cDNA library was constructed from *N. benthamiana* leaves. Using GAL4-based yeast-two hybrid system, we screened 3.3×10^6 independent yeast transformants using PVX CP as a bait and finally identified six different positive candidate clones showing activity of reporter genes *HIS3*, *ADE2*, and *lacZ* on selection medium. One positive clone was selected for further analysis. Sequence analysis revealed that the selected cDNA clone encode a plant-specific protein with homologue in *N. tabacum* and termed as *NbPCIP1*. Interestingly, a cDNA clone different from *NbPCIP1* but highly similar to *NbPCIP1* was isolated and subsequently named as *NbPCIP2* (89.5% sequence identity). As shown in Fig. 1, both *NbPCIP1* and *NbPCIP2* were 456 bp in length and contained one ORF encoding 151 amino acids (aa).

The sequence alignment of deduced amino acid showed that *NbPCIP1* and *NbPCIP2* shared high amino acid sequence identity to *Tomato mosaic virus* (ToMV) CP interacting protein-L (*IP-L*; GenBank Acc. No. AB040409) of *N. tabacum* protein (89% and 81%, respectively). Interestingly, IP-L has been reported as putative ToMV CP responsive protein of *N. tabacum* and facilitated long-distance movement of ToMV in *N. tabacum* (Li et al., 2005). *NbPCIP1* and *NbPCIP2* also showed high sequence identity to the senescence up-regulated gene (*SlSENU1*; GenBank Acc. No. CAA99759) of *Solanum lycopersicon* protein (58.5% and 59.3%, respectively) and to *CaSENU1* (GenBank Acc. No. AY479987.1) of *Capsicum annuum* protein (42.4% and 43.4%, respectively) and relatively low sequence identity to the glycine-rich protein (*AtGRP*; GenBank Acc. No. BAF00139) of *Arabidopsis thaliana* protein (22% and 18%, respectively) and *OsGRP-1* (GenBank Acc. No. P0C5C7) of *Oryza sativa* protein (17.8% and 23.7%, respectively). Prediction of subcellular localization signals in NbPCIP1 and NbPCIP2 using 'PSORT' software (http://123genomics.com; Nakai and Horton, 2007) revealed an ER membrane retention signal-like motif at the C-terminus. NbPCIP1, NbPCIP2 and IP-L contain the KDLE motif while
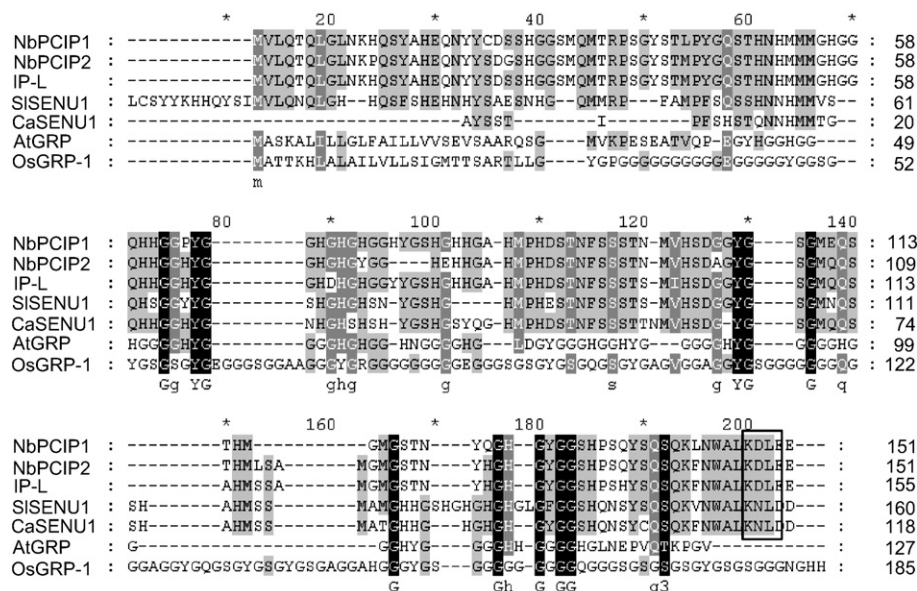

Fig. 1. Alignment of predicted amino acid sequences of the NbPCIPs and the other possible orthologs. The amino acids are represented by single letter amino acid codes. Alignment was generated using CLUSTAL W program (DNAStar, USA). The tentative superposition of the conserved ER membrane retention motifs is boxed. GenBank accession numbers are as follows: *IP-L*, ToMV CP interacting protein-L coding gene of *N. tabacum* (AB040409); *SlSENU1*, senescence up-regulated gene of *Solanum Lycopersicon* (CAA99759); *CaSENU1*, SENU1 gene of *Capsicum annum* (AY479987.1); *AtGRP*, Glycine-rich protein (GRP) coding gene of *Arabidopsis thaliana* (BAF00139); *OsGRP-1*, GRP-1 gene of *Oryza sativa* (P0C5C7).

SISENU1 and CaSENU1 contain the KNLD motif at the C-terminus as an ER membrane retention signal-like motif (Fig. 1, ER membrane retention signal-like motif are boxed).

PVX CP interacts with NbPCIP1 but not NbPCIP2 in yeast

To confirm whether the both NbPCIP1 and NbPCIP2 interact with PVX CP in yeast, we carried out a yeast-two hybrid assay. Each full-length *NbPCIP1* and *NbPCIP2* was cloned into pACT2 vector (pPCIP1-AD and pPCIP2-AD, respectively) and the full-length PVX CP gene was inserted into the GAL4 DNA-binding domain vector pAS2-1 (pPVX CP-BD). These clones were co-transformed into *Saccharomyces cerevisiae* strain AH109. As shown in Fig. 2A, we confirmed that AH109 co-transformed with pNbPCIP1-AD and pPVX CP-BD did grow on SD medium lacking leucine, tryptophan, histidine and adenine (−LWHA) while AH109 co-transformed with pAS2-1 (BD) and pNbPCIP1-AD or pPVX CP-BD and pACT2 (AD) did not (Fig. 2A). The ToMV CP interacting with *N. tabacum IP-L* (Li et al., 2005) was used as an additional control (pToMV CP-BD) to determine its interaction with NbPCIP1. As shown in Fig. 2A, AH109 co-transformed with pNbPCIP1-AD and pToMV CP-BD also grew on SD-LWHA. Neither pPCIP1-AD (prey) nor pPVX CP-BD (bait) alone activated *HIS3*, *ADE2* or *lacZ* reporter genes (data not shown). These results were further confirmed by quantitative β-galactosidase filter assays using o-nitrophenyl-β-D-galactopyranoside (ONPG) as substrate and showed the results like that of yeast on selection medium (Fig. 2A). These results revealed that NbPCIP1 interacted with PVX CP and ToMV CP in yeast while no interaction was observed between PVX CP and NbPCIP2.

NbPCIP1 interacts with PVX CP in vitro and in planta

To verify the interaction of NbPCIP1 with PVX CP identified by the two-hybrid system, an independent *in vitro* protein binding assay was employed. NbPCIP1 was expressed as maltose-binding protein (MBP) fusion (NbPCIP1-MBP) in *E. coli* cells and coupled to an amylose affinity resin. After incubation with His-tagged PVX CP (PVX CP-His), resin bound protein complexes were eluted and subsequently analyzed for the presence of PVX CP-His and NbPCIP1-MBP by western blot analysis with anti-PVX CP antibodies and anti-MBP monoclonal antibodies, respectively. As shown in Fig. 2, NbPCIP1-MBP bound to PVX CP-His (lane 4), while MBP used as negative control did not (lane 5). These results demonstrate that NbPCIP1 interacts directly with PVX CP.

Specific interaction of NbPCIP1 with PVX CP in yeast and *in vitro* further suggests their interaction and functional significance. To further confirm the interaction of NbPCIP1 with PVX CP, we conducted bimolecular fluorescent complementation (BiFC) assay in *Agrobacterium*-infiltrated *N. benthamiana* plants and observed yellow fluorescent protein (YFP) fluorescence signals by epifluorescence microscope (Carl Zeiss, Inc., Germany). BiFC assay has emerged as one of the most promising techniques for detection of protein binding *in vivo* and is a very sensitive method for detecting protein–protein interactions (Morell et al., 2008). To perform this assay in a *N. benthamiana* plant, NbPCIP1 and NbPCIP2 were fused to the N-terminal YFP fragment (NYFP) and PVX CP, ToMV CP and *Cucumber mosaic virus* (CMV) CP were fused to the C-terminal YFP fragment (CYFP) (Fig. 3A). Co-expression of NYFP-fused NbPCIP1 (pNbPCIP1-NYFP) and CYFP-fused PVX CP (pPVX CP-CYFP) induced YFP fluorescence signals in agro-infiltrated *N. benthamiana* epidermal cells (Fig. 3E). However, YFP fluorescence was not observed in NYFP + CYFP, NbPCIP1-NYFP + CYFP, and NYFP + PVX-CP-CYFP-expressed *N. benthamiana* epidermal cells (Fig. 3, panels B–D, respectively). Co-expression of NbPCIP2-NYFP and PVX CP-CYFP induced YFP fluorescence signals significantly weaker than that observed from the interaction between NbPCIP1-NYFP and PVX CP-CYFP in agro-infiltrated *N. benthamiana* epidermal cells (Fig. 3H). Since ToMV CP was found to interact with NbPCIP1 in yeast, we used pToMV CP-CYFP as positive control. Again, co-expression of NYFP-
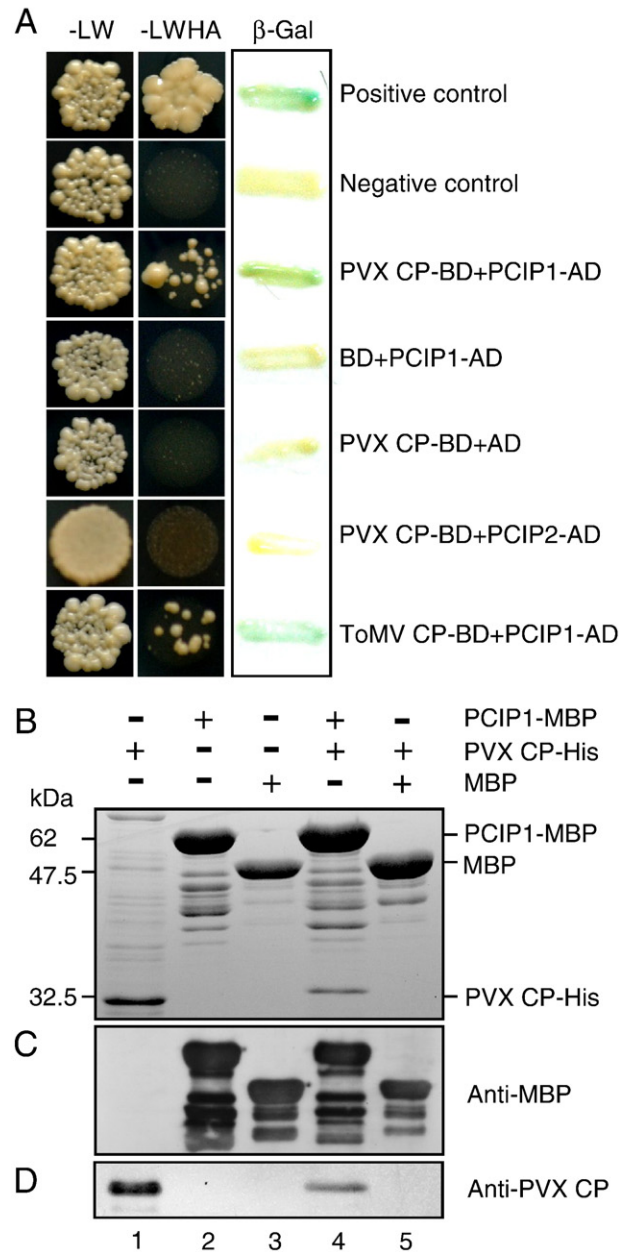

Fig. 2. Interactions between NbPCIPs and PVX CP. (A) Interactions of NbPCIPs and PVX CP using yeast-two hybrid assay and β-galactosidase filter assay. Plasmids (pTD1-1 + pVA3-1, positive control; pTD1-1 + pLAM5′, negative control; pPVX CP-BD + pNbPCIP1-AD; pBD + pNbPCIP1-AD; pPVX CP-BD + pAD; pPVX CP-BD + pNbPCIP2-AD; pToMV CP-BD + pNbPCIP1-AD) for yeast-two hybrid assay were transformed into yeast AH109, according to the manufacturer's instruction. Yeast cells transformed with bait and prey vector were grown on SD-Leu⁻/Trp⁻/His⁻/Ade⁻ (right panel) and SD-Leu⁻/Trp⁻ (left panel) medium, respectively. lacZ activity was tested using β-galactosidase filter assay (β-Gal). (B–D) *E. coli* expression of NbPCIP1-MBP and PVX CP-His and their *in vitro* interaction. His-tagged PVX CP (PVX CP-His), MBP fused NbPCIP1 (NbPCIP1-MBP), and MBP were expressed in *E. coli* strain BL21-DE3 and coupled to a Ni⁺⁺ resin (PVX CP-His) and an amylase matrix (NbPCIP1-MBP and MBP). In lanes 4 and 5, purified NbPCIP1-MBP and MBP were pre-incubated with 100 μg of affinity-purified His-tagged PVX CP, washed, and centrifuged for 5 min. The pellets were then separated by 12% SDS-PAGE and stained by Coomassie blue staining (B) or blotted onto PVDF membranes. The blots were probed with anti-PVX CP antibody (D) or anti-MBP monoclonal antibody (C). The positions of the molecular mass markers are shown on the left of panel B.

fused NbPCIP1 (pNbPCIP1-NYFP) and CYFP-fused ToMV CP (pToMV CP-CYFP) induced YFP fluorescence signals in agro-infiltrated *N. benthamiana* epidermal cells (Fig. 3G). As expected, significantly weaker fluorescence signals were observed from NbPCIP2-NYFP and ToMV CP-CYFP infiltrated *N. benthamiana* epidermal cells (Fig. 3J). To
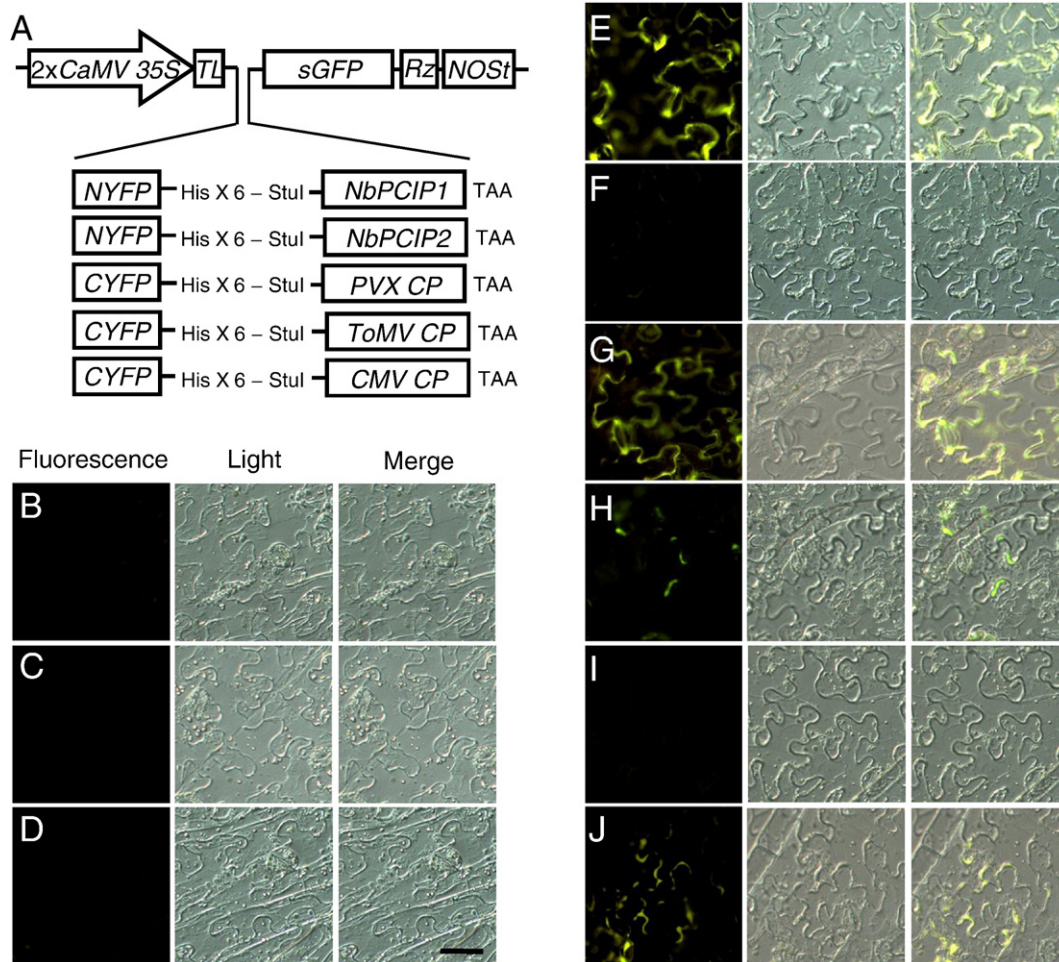
Fig. 3. Interactions of NbPCIPs and PVX CP by BiFC assay *in planta*. (A) Schematic representation of constructs used for BiFC assay. Complete NbPCIP1, NbPCIP2, PVX CP, ToMV CP, and CMV CP were fused to the C- and N-terminal of YFP (CYFP and NYFP, respectively) sequence with stop codon (TAA) at the 3′ end of each ORF in the modified pZP212 vector. Plasmids were agro-infiltrated in *N. benthamiana* leaves, and the reconstructed YFP signal was detected in the epidermal cell layer by epifluorescence microscopy. Co-expression of NYFP + CYFP (B), NbPCIP1-NYFP + CYFP (C), NYFP + PVX CP-CYFP (D), NbPCIP1-NYFP + PVX CP-CYFP (E), NbPCIP1-NYFP + CMV CP-CYFP (F), NbPCIP1-NYFP + ToMV CP-CYFP (G), NbPCIP2-NYFP + PVX CP-CYFP (H), NbPCIP2-NYFP + CMV CP-CYFP (I), and NbPCIP2-NYFP + ToMV CP-CYFP (J) shows specific YFP complementation by NbPCIP1-NYFP + PVX CP-CYFP and NbPCIP1-NYFP + ToMV CP-CYFP interactions. NbPCIP2-NYFP weakly interacts with PVX CP-CYFP and ToMV CP-CYFP, but significantly less, *in planta*. pCMV-CYFP and pToMV CP were used for negative and positive controls, respectively. YFP-derived fluorescent signals of single confocal sections (left), the transmission mode (middle), and the superimposed image (right) were shown. Bars denote 20 μm.

determine the specificity of NbPCIP1 interaction with viral CPs, pCMV CP-CYFP was used. YFP fluorescence was observed neither in pNbPCIP1-NYFP + pCMV CP-CYFP nor pNbPCIP2-NYFP + pCMV CP-CYFP-expressed *N. benthamiana* epidermal cells (Figs. 3F and I, respectively). These results provided additional evidence supporting strong interaction of NbPCIP1 with PVX CP or ToMV CP in plant cells. In contrast, significantly weak interactions between NbPCIP2 and PVX CP or ToMV CP were observed *in planta*. Our results also suggested that the interaction between NbPCIP1 and PVX CP is not due to the fact that the CP is just being sticky since it did not interact with CMV CP.

Existence of PVX affects expression levels of NbPCIP1 mRNA in plants

To determine if there were any differences in the expression level of *NbPCIP1* mRNA in mock-inoculated and PVX-infected *N. benthamiana* leaves, we carried out quantitative real-time polymerase chain reaction (qRT-PCR). Total RNAs were isolated from mock-inoculated and PVX-infected *N. benthamiana* leaves at 0, 1, 6, 9, 12, 24, 36, 48, and 72 h post inoculation (hpi), respectively, and subsequently analyzed for *NbPCIP1* mRNA accumulation as described previously (Park et al., 2008a, 2008b). Although there was variation among the individual samples at each time points, it was obvious that a small amount of *NbPCIP1* mRNAs was accumulated both in mock and PVX-infected *N.*

benthamiana plants till 9 hpi and then abundances of *NbPCIP1* mRNAs were significantly increased from 12 hpi both in mock and PVX-infected leaves till 72 hpi. However, we could verifiy that *NbPCIP1* mRNAs are more increased from 24 to 48 hpi in PVX-infected plants as compared to that in mock-inoculated control leaves (Fig. 4A). We then carried out qRT-PCR using previously synthesized cDNAs from PVX-infected *N. benthamiana* leaves for detection of PVX RNA accumulation. Accumulation of PVX RNA was increased dramatically from 24 hpi (Fig. 4B). To further confirm our experimental data, we also included one of heat shock protein 70 (Hsp70c-1) as an external control gene. Expression of *Hsp70c-1* was found to be induced by PVX infection (Chen et al., 2008). As shown in Fig. 4C, semi-quantitative RT-PCR showed that the expression level of the cytoplasmic *Hsp70c-1* was also enhanced by PVX infection. These results indicate that expression of NbPCIP1 is increased by PVX infection in the early stage of virus infection and when the expression of NbPCIP1 came to its peak, accumulation of PVX RNA is also significantly increased.

Co-localization of NbPCIP1-sGFP and PVX CP-RFP in N. benthamiana protoplasts and epidermal cells

To confirm the subcellular localization of NbPCIP1 on *N. benthamiana* leaves, we fused the green fluorescent protein (sGFP)
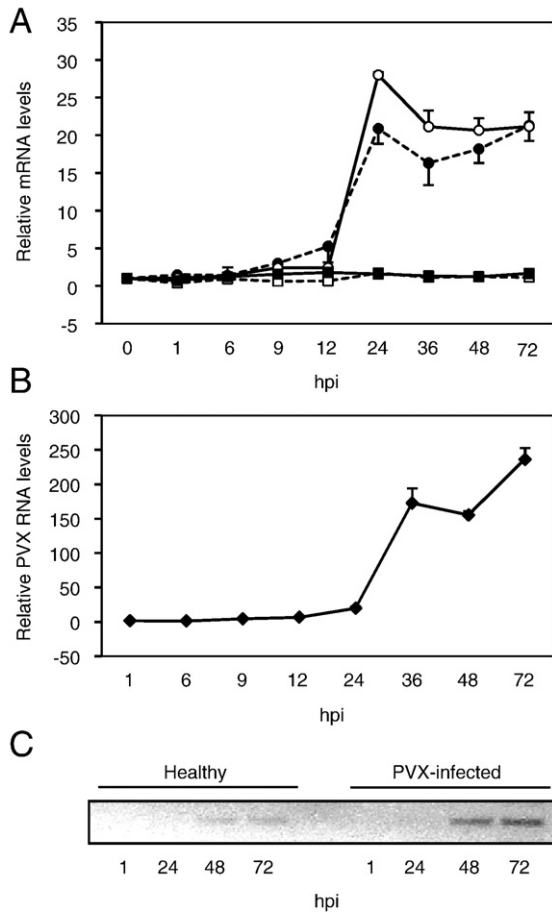
Fig. 4. Accumulation of *NbPCIP1* mRNA and PVX RNA in healthy and virus infected *N. benthamiana* plants. (A) Comparison of relative *NbPCIP1* mRNA levels in healthy (●) and PVX-inoculated (○) *N. benthamiana* plants. *N. benthamiana* leaves were harvested at 0, 1, 6, 9, 12, 24, 36, 48, and 72 hours post inoculation (hpi). Total RNAs were extracted from harvested leaves and utilized for cDNA synthesis. Relative *NbPCIP1* mRNA levels were assayed by qRT-PCR as described in Materials and methods. Accumulation of *EF-1* mRNA, as endogenous gene, in healthy (□) and PVX-inoculated (■) *N. benthamiana* plants used for negative control. (B) PVX RNA accumulation in *N. benthamiana* leaves. Total RNAs, which were extracted from PVX-infected leaves for detection of *NbPCIP1* mRNA, were utilized for cDNA synthesis using specific PVX CP primer (Table 3). Relative PVX RNA levels (♦) were assayed by qRT-PCR as described in Materials and methods. Each value is the mean with standard error compiled from six independent experiments. (C) Accumulation of *Hsp70c-1* mRNA. Induction of *Hsp70c-1* mRNA by PVX infection was observed as previously described (Chen et al., 2008). Each sample at 0, 24, 48, and 72 hpi were amplified by PCR using specific primer set (Table 3) using synthesized cDNAs from mock-inoculated (Healthy) and PVX-infected plants (PVX-infected), respectively. The bands were separated on an 1% agarose gel and visualized by staining with Et-Br.

epidermal cells of agro-infiltrated leaves and observed similar localization of each protein as compared to those from protoplasts experiment (data not shown).

To determine whether the localization of NbPCIP1 in granular-like structures is associated with ER as predicted from sequence analysis using 'PSORT' software (http://123genomics.com, Nakai and Horton, 2007), we observed accurate localization of NbPCIP1-sGFP after co-expression with Histidine–Aspartate–Glutamtae–Leucine (HDEL)-ER retention signal-contained marker (pRFP-ER; Chakrabarty et al., 2007) on *N. benthamiana* leaf epidermal cells (Fig. 7). The co-expression of ER marker and NbPCIP1-sGFP revealed that NbPCIP1-sGFP is associated at ER (Fig. 7C, ER associated-NbPCIP1s-sGFP are marked in arrow).

To determine if the presence of PVX CP might alter the subcellular localization of NbPCIP1, we carried out co-expression of RFP-fused PVX CP (PVX CP-RFP) and NbPCIP1-sGFP in *N. benthamiana* leaves using an agro-infiltration method, prepared protoplasts and epidermal cells from co-expressed *N. benthamiana*
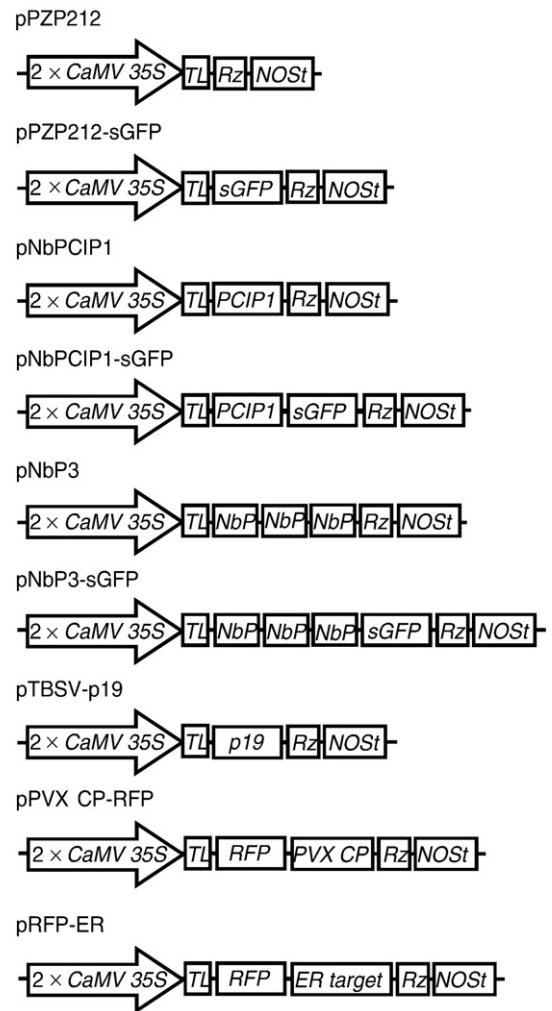

Fig. 5. Schematic representation of transient over-expression and gene silencing constructs used for agro-infiltration of *N. benthamiana*. NbPCIP1 and three copies of the partial NbPCIP1 fragments were fused to the pPZP212 and pPZP212-sGFP constructs (pNbPCIP1, pNbPCIP1-sGFP, pNbP3, and pNbP3-sGFP). The pPZP212-sGFP contains sGFP gene under control of *Tobacco etch virus* (TEV) leader sequence (TL) in the pPZP212 vector. PVX CP fragment was fused to the pSITE-4CA vector (PVX CP-RFP). pNbPCIP1, pNbPCIP1-sGFP, and PVX CP-RFP were prepared for transient over-expression assay. pTBSV-p19 construct was used as gene silencing suppressor for over-expression analysis. pNbP3 and pNbP3-sGFP were used for silencing of NbPCIP1. pRFP-ER containing Histidine–Aspartate–Glutamtae–Leucine (HDEL)-ER retention signal (Chakrabarty et al., 2007) was used for subcellular ER localization study.

in NbPCIP1 (pNbPCIP1-sGFP) as shown in Fig. 5. We utilized agro-infiltration to deliver pNbPCIP1-sGFP, pTBSV-p19 as a silencing suppressor, and pPZP212-sGFP as a control into the cells of *N. benthamiana* leaves. We collected the agro-infiltrated leaves at 3 days after agro-infiltration and extracted protoplasts from agro-infiltrated *N. benthamiana* leaves. The protoplasts were observed for GFP fluorescence signal by epifluorescence microscope, respectively. We could observe that NbPCIP1-sGFP associated with granular-like structures throughout the cytoplasm in *N. benthamiana* protoplasts (Figs. 6E to G), whereas sGFP-expressed from pPZP212-sGFP were shown to distribute in a diffuse manner throughout the cytoplasm and nucleus (Figs. 6A to C). Similarly, PVX CP-RFP distributed in punctuate structures throughout the cytoplasm when expressed alone (Figs. 6I to K). To make sure that the processes of making protoplasts did not affect localization of pPZP212-sGFP or PVX CP-RFP, we examined localization of pPZP212-sGFP and PVX CP-RFP in
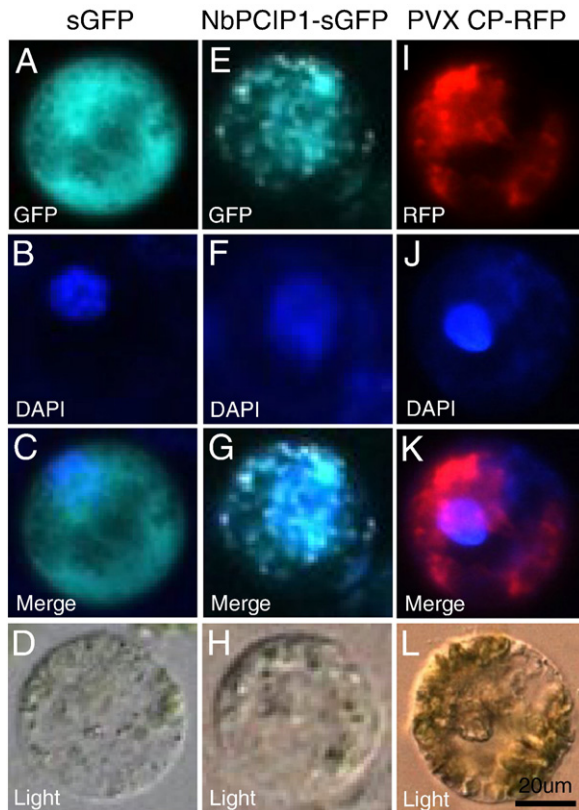
sGFP NbPCIP1-sGFP PVX CP-RFP

Fig. 6. Subcellular localization of NbPCIP1 and PVX CP in *N. benthamiana* protoplasts. Localization of pPZP212-sGFP (sGFP) as a positive control (A–D), NbPCIP1-sGFP (E–H), and PVX CP-RFP (I–L), respectively, in *N. benthamiana* protoplasts. Protoplasts were observed under the green channel (A and E), red channel (I), and light channel (D, H, and L) by epifluorescence microscope. The nucleus was stained by 4′-6′-Diamidino-2-phenylindole (DAPI) staining dye (B, F, and J). Overlay of GFP signal and DAPI staining images or RFP signal and DAPI staining images show in C, G, and K, respectively.

at 3 day after agro-infiltration, and observed GFP and RFP fluorescence signals by epifluorescence microscope. The result shows that the NbPCIP1-sGFP in the presence of PVX CP-RFP was localized in an inclusion body-like complex in areas surrounding the nucleus (Figs. 8A and B, a–c) and PVX CP-RFP was also localized in same area where NbPCIP1-sGFP was localized (Figs. 8A and B, d and e). Altogether, these results suggest that PVX CP was distributed in the cytoplasm of cells whereas NbPCIP1 was associated mainly with ER. When NbPCIP1 was co-expressed with PVX CP, however, NbPCIP1 co-localized with PVX CP as inclusion body-like complexes in areas surrounding the nucleus.

NbPCIP1 positively affects PVX replication in N. benthamiana plants

To examine the functional role of NbPCIP1 to PVX RNA replication in *N. benthamiana* plants, we utilized pNbPCIP1-sGFP and pTBSV-p19 constructs (Fig. 5) for transient over-expression assay. We carried out agro-infiltration in *N. benthamiana* leaves and detected accumulation levels of *NbPCIP1* mRNA in NbPCIP1 over-expressed and mock *N. benthamiana* leaves using qRT-PCR. As shown in Fig. 9A and Table 1, accumulation of *NbPCIP1* mRNA in NbPCIP1 over-expressed leaves increased approximately twenty times as compared to that of mock plants at 3 days post agro-infiltration (dpi). We observed that the level of *NbPCIP1* mRNA in NbPCIP1 over-expressed leaves was maintained at least ten times the over-expressed level during 3–5 dpi as confirmed by qRT-PCR (Fig. 9A and Table 1). Therefore, we carried out PVX-challenge

inoculation at 3 dpi on both mock (pPZP212-sGFP + pTBSV-p19) and over-expressed (pNbPCIP1-sGFP + pTBSV-p19) leaves. PVX-challenge inoculated leaves were harvested at 1 and 2 days post challenge inoculation (dpci), respectively, and extracted total RNA for cDNA synthesis. By qRT-PCR, we compared the PVX RNA accumulation in NbPCIP1 over-expressed leaves with that on mock leaves. As shown in Fig. 9C and Table 2, we observed that PVX RNA accumulation was remarkably increased (approximately eight or more times at both time points) as compared to that in control leaves. These results indicate that the over-expression of NbPCIP1 positively affects PVX RNA replication in *N. benthamiana* plants.

To further examine the possible role of NbPCIP1 on PVX RNA replication in *N. benthamiana* plants, we utilized TRV-based VIGS system for silencing of *NbPCIP1*. However, when the silenced plants were challenge with PVX, co-infection of *N. benthamiana* plants with TRV and PVX caused a synergistic symptom due to incomplete silencing and thus replication of TRV vectors (data not shown). Therefore, we decided to utilize transgene silencing assay. According to the previous report on transgene silencing, a transgene with three or four repeats induced efficient gene silencing of the primary plants (Ma and Mitra, 2002). For this reason, to cause high frequency gene silencing, three copies of the partial NbPCIP1 gene were tandemly fused to the modified pPZP212-sGFP vector (pNbP3; Fig. 5). We carried out agro-infiltration in *N. benthamiana* leaves and detected accumulation levels of *NbPCIP1* mRNA in upper leaves of NbPCIP1-silenced and mock *N. benthamiana* plants using qRT-PCR at
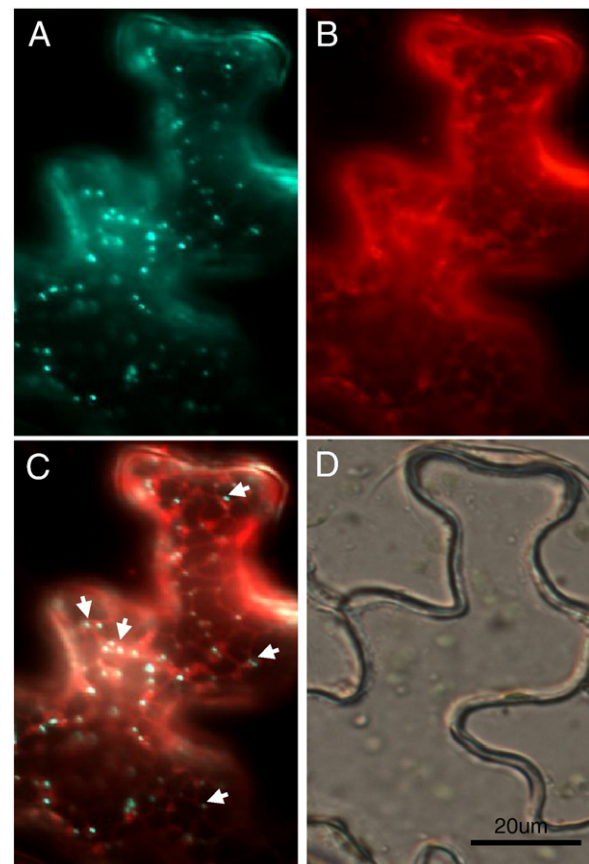

Fig. 7. Subcellular localization of NbPCIP1-sGFP in ER or ER-associated granular-like structure of *N. benthamiana* epidermal cells. Epidermal cells were observed under the green channel (A), red channel (B), and light channel (D), respectively. GFP fluorescence signals of NbPCIP1-sGFP shows granular-like structure under the green channel (A) and RFP fluorescence signals of RFP-ER shows in the ER under the red channel (B) by fluorescence epimicroscope. Overlay of GFP and RFP signal images show in C. Bar in panel D denotes 20 μm.
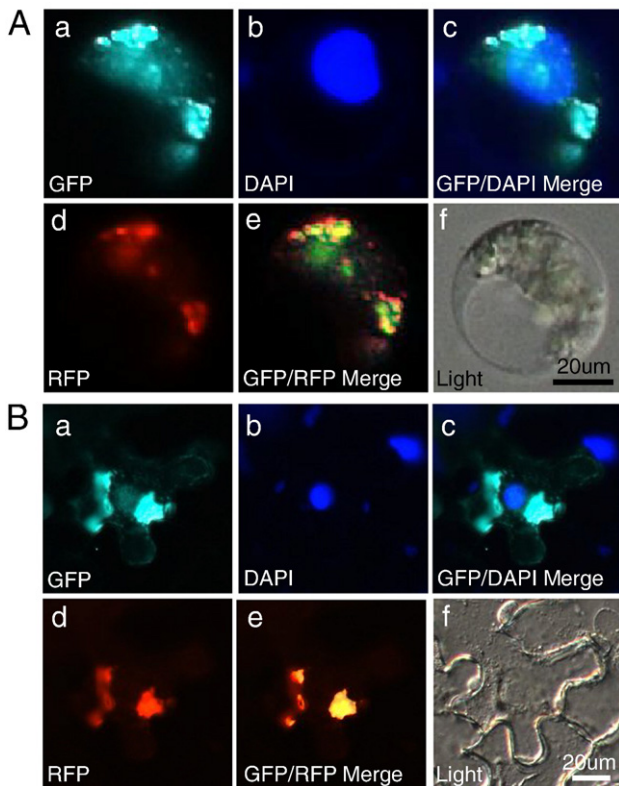
Fig. 8. Co-localization of NbPCIP1-sGFP and PVX CP-RFP in *N. benthamiana* protoplasts (A) and epidermal cells (B). pNbPCIP1-sGFP and pPVX CP-RFP transformed *A. tumefaciens* strain GV2260 were co-infiltrated into *N. benthamiana*. Protoplasts and epidermal cells from co-expressed leaves were observed under the green channel (GFP; a), red channel (RFP; d), and light channel (Light; g). The nucleus was stained by DAPI staining dye (DAPI; b). Overlay of sGFP signal and DAPI staining images or RFP and sGFP signal images show in c and e (GFP/DAPI Merge and GFP/RFP Merge), respectively. Bars denote 20 μm.

NbPCIP1 positively affect not only PVX RNA replication but also virus movement.

NbPCIP1 affects viral movement in N. benthamiana plants

According to the previous reports, potexviruses required CP for cell-to-cell movement (Morozov and Solovyev, 2003; Verchot-Lubicz, 2005). We found that NbPCIP1 affects PVX RNA accumulation in *N. benthamiana* plants by transient over-expression and transgene silencing assay. We thought that viral movement might also be affected by PVX RNA accumulation and thus observed PVX movement on NbPCIP1 over-expressed and silenced *N. benthamiana* plants upon PVX-challenge inoculation assay with sGPF expressing PVX infectious clone (pSPVX-sGFP; Fig. 11A). pSPVX-sGFP was challenge inoculated in NbPCIP1 over-expressed (pNbPCIP1 + pTBSV-p19) and silenced (pNbP3) *N. benthamiana* leaves along with control (pPZP212 + pTBSV-p19 and pPZP212 for over-expression and silencing experiments, respectively) plants at 3 and 11 dpi, respectively, by agro-infiltration method. At 5 dpi, *N. benthamiana* plants were observed under the Hand UV Lamp (Figs. 11D to G). In NbPCIP1 over-expressed *N. benthamiana* leaves, PVX more systemically spread to upper uninoculated leaves than in that of mock (Figs. 11B, D, and E). In contrast, PVX movement was delayed on NbPCIP1-
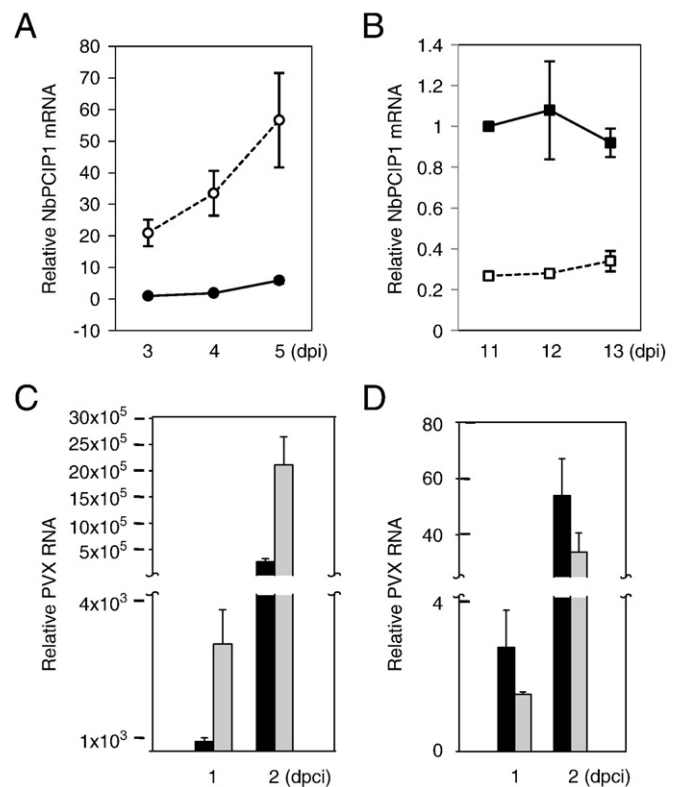
11 dpi. As shown in Fig. 9B and Table 1, silencing efficiency of *NbPCIP1* mRNA in NbPCIP1-silenced upper leaves was approximately 70% in *N. benthamiana* plants. We, therefore, carried out PVX-challenge inoculation on silenced upper leaves at 11 dpi. PVX-challenge inoculated leaves were harvested at 1 and 2 dpci, respectively, and analyzed for PVX RNA accumulation. By conducting qRT-PCR, we compared the PVX RNA accumulation in upper leaves of NbPCIP1-silenced plants with that in control plant. The accumulation of PVX RNA was decreased approximately 46% and 37% in silenced upper leaves at 1 and 2 dpci, respectively, as compared to that on upper leaves of control plants (Fig. 9D and Table 2). Altogether, these data supports that a lack of NbPCIP1 negatively affect PVX RNA replication.

To determine the effect of NbPCIP1 over-expression and silencing on symptom development, we observed phenotype changes of NbPCIP1 over-expressed and silenced plants after PVX challenge inoculations. NbPCIP1 over-expressed plants showed severe necrosis after virus infection (Fig. 10A). Interestingly, NbPCIP1 over-expressed plants also developed a wilting type symptom even by buffer inoculation (Fig. 10B). In contrast, no significant phenotype difference was observed on NbPCIP1 silenced leaves either by PVX infection or buffer inoculation (Figs. 10C and 10D, respectively). We, however, observed the appearance of mild mosaic symptom in the NbPCIP1-silenced upper leaves (Fig. 10F) while the severe mosaic symptom was developed in upper leaves of control plants (Fig. 10E). This result suggests that the silencing of *NbPCIP1* could delay the development of systemic symptoms upon PVX infection. Altogether, these data support that the presence of

Fig. 9. *NbPCIP1* mRNA and PVX RNA accumulation in NbPCIP1 over-expressed and silenced *N. benthamiana* plants. (A and B) Accumulation of *NbPCIP1* mRNA in over-expressed and silenced *N. benthamiana* plants. Accumulation of *NbPCIP1* mRNA was measured by qRT-PCR at 3–5 days after transient over-expression (panel A, ○) or at 11–13 days post silencing (panel B, □) and compared to those in control plants (pPZP212-sGFP and pTBSV-p19 for over-expression, ●; pPZP212-sGFP for silencing, ■). (C and D) Effect of NbPCIP1 over-expression and silencing on PVX RNA accumulation. PVX-challenge inoculation was performed at 3 and 11 days after over-expression and silencing infiltrations, respectively. Challenge-inoculated *N. benthamiana* leaves were harvested at 1 and 2 days post challenge inoculation (dpci) and analyzed for PVX RNA accumulation using qRT-PCR. The closed and shaded bars represent PVX RNA accumulations on control and NbPCIP1 over-expressed (C) or silenced (D) leaves, respectively. Each value is the mean compared to that of the control and the standard error compiled from at least six independent experiments.

Table 1
NbPCIP1 mRNA accumulation in NbPCIP1 over-expressed and silenced *N. benthamiana* leaves

Dpi	Mock		Over-expression		Dpi	Mock		Silencing	
	AVE[a]	ST-error	AVE[a]	ST-error		AVE[a]	ST-error	AVE[a]	ST-error
3	1.00c	±0.00	20.98bc	±4.18	11	1.00a	±0.00	0.27b	±0.01
4	1.91c	±0.13	33.49b	±7.08	12	1.08a	±0.24	0.28b	±0.02
5	5.89c	±0.93	56.64a	±14.89	13	0.92a	±0.07	0.34b	±0.05

Means with the same letter are not significantly different at $P \leq 0.05$. AVE and ST-error represent average and standard error, respectively.
 [a] Data were analyzed by ANOVA and means were compared using the Fisher's LSD test using SAS program (Version 9.1).

silenced *N. benthamiana* plants compared to that in control (Figs. 11C, F, and G). The results indicated that NbPCIP1 affects viral movement in *N. benthamiana* plants.

Discussion

We have identified NbPCIP1 that interacts with PVX CP from an *N. benthamiana* cDNA library using yeast-two hybrid assay and verified that NbPCIP1 specifically interacts with PVX CP in yeast, *in vitro*, and in plant cell by yeast-two hybrid assay, *in vitro* protein binding assay, and BiFC assay, respectively (Figs. 2 and 3). Functional significance of this interaction was examined by virus challenge inoculation in transient NbPCIP1 over-expressed and silenced *N. benthamiana* plants. Progeny viral RNA analyses on these plants revealed that transient over-expression of NbPCIP1 on *N. benthamiana* plants caused increased accumulation of PVX RNA (Fig. 9C and Table 2). On the other hand, the accumulation levels of PVX RNA decreased significantly in NbPCIP1-silenced *N. benthamiana* plants as compared to that of control plants (Fig. 9D and Table 2). Therefore, it can be concluded that the NbPCIP1 is interacting with the PVX CP and affects viral RNA replication directly and/or indirectly.

The amino acid sequence identity between NbPCIP1 and NbPCIP2 is approximately 89%. The main difference between them is the presence (HYGS residues) of a 75–78 aa region in NbPCIP1 that is absent in NbPCIP2 and the absence of a 112–115 aa region in NbPCIP1 that is present (LSAM residues) in NbPCIP2 (Fig. 1). Although the amino acid sequence identity between NbPCIP1 and NbPCIP2 was very high, we observed that only NbPCIP1 interacts with PVX CP in our assays including yeast-two hybrid assay and β-galactosidase filter assay (Fig. 2A). As shown in Fig. 1, the deduced amino acid sequence of NbPCIP1 also showed high sequence identity to that of ToMV CP-interacting protein-L (IP-L) identified from *N. tabacum* (Fig. 1). Recently, it has been reported that IP-L may affect chloroplast function and stability and thus lead to chlorosis in ToMV infected *N. tabacum* (Zhang et al., 2008). We observed the interaction of NbPCIP1 with ToMV CP in yeast two-hybrid assay (Fig. 2A) and in BiFC assay (Fig. 3G). Interestingly, the above mentioned HYGS residues are only present in NbPCIP1 but not in NbPCIP2 and are also present in IP-L as YYGS. Since the other residues are present only in NbPCIP2 at 112–115 (LSAM) and are also present in IP-L as SSAM, we speculate that aa residues located at 75–78 might be responsible for determining the sequence limitation of the interaction between NbPCIP1 and PVX CP.
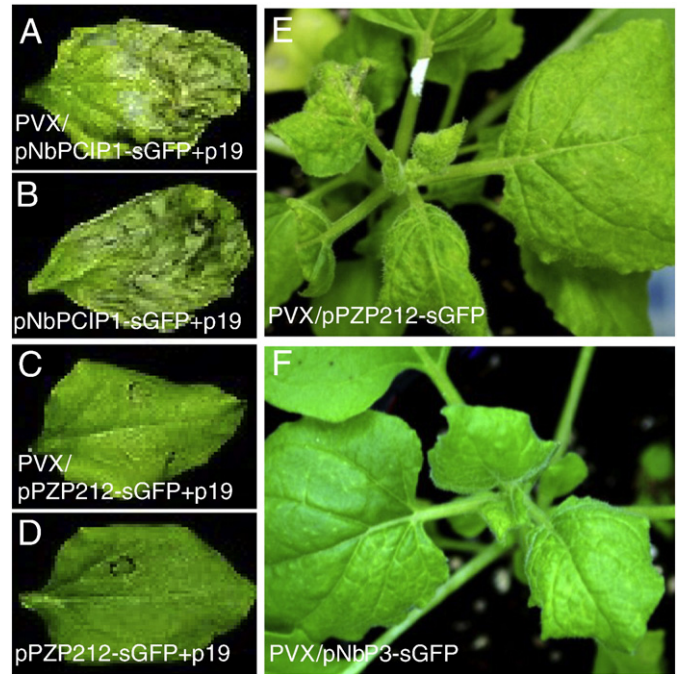

Fig. 10. Symptom development of PVX-challenged inoculated plants in NbPCIP1 over-expressed and silenced *N. benthamiana* plants. NbPCIP1 was either over-expressed (A and B) or silenced (E and F) in *N. benthamiana* plants as described in Materials and methods and in Fig. 7 legend. The pPZP212-sGFP was used as an over-expression control (C and D). Each *N. benthamiana* plant was challenge inoculated with either PVX (A, C, E, and F) or buffer (B and D). (A–D) Symptom development was observed at 2 dpci to determine the effect of NbPCIP1 over-expression compared to that of control. Severe necrosis and/or wilting symptom were obvious on NbPCIP1 over-expressed leaves (A and B). (E and F) Development of PVX-challenge inoculation induced symptoms in NbPCIP1-silenced *N. benthamiana* plant (F) compared to control (E) at 14 dpi. A mild mosaic symptom was observed in silenced plant while severe mosaic and necrosis were observed in control plant.

In this regard, it might be worth mentioning the results of BiFC assays showing the significantly weak interaction of NbPCIP2 with PVX CP and ToMV CP *in planta* (Figs. 3, panel H and J). Since we observed interaction, although it was significantly weak, it is possible that the other amino acid residue(s) might also contribute to the interaction between PVX CP and NbPCIPs. Further research is required to reveal the importance of these residues in interaction PVX CP.

NbPCIPs also showed relatively high aa sequence identity with SlSENU1 and CaSENU1 (Fig. 1). John et al. (1997) reported that the mRNA levels of *SlSENU1* increased during leaf senescence and *Sl-SENU1* was expressed at high levels during leaf development and in other plant organs. When we determined the *NbPCIP1* mRNA expression levels in healthy *N. benthamiana* plants, we observed that the *NbPCIP1* mRNA accumulation was increased over the time (Fig. 4A). In addition, the NbPCIP1 over-expressed *N. benthamiana* leaves are easily wilted by slight physical stress and by virus infection as compared to those of control plants (Figs. 10A to D). These results prompted us to speculate that *NbPCIPs* may also function as senescence-related gene. It remains to be determined whether

Table 2
PVX RNA accumulation in NbPCIP1 over-expressed and silenced *N. benthamiana* leaves

Dpi	Mock		Over-expression		Mock		Silencing	
	AVE[a]	ST-error	AVE[a]	ST-error	AVE[a]	ST-error	AVE[a]	ST-error
1	364.46b	±144.01	4093.00b	±1311.02	2.68c	±0.96	1.47c	±0.06
2	265161.10b	±60219.00	2110213.00a	±539275.20	53.84a	±13.16	33.94b	±6.75

Means with the same letter are not significantly different at $P \leq 0.05$. AVE and ST-error represent average and standard error, respectively.
 [a] Data were analyzed by ANOVA and means were compared using the Fisher's LSD test using SAS program (Version 9.1).
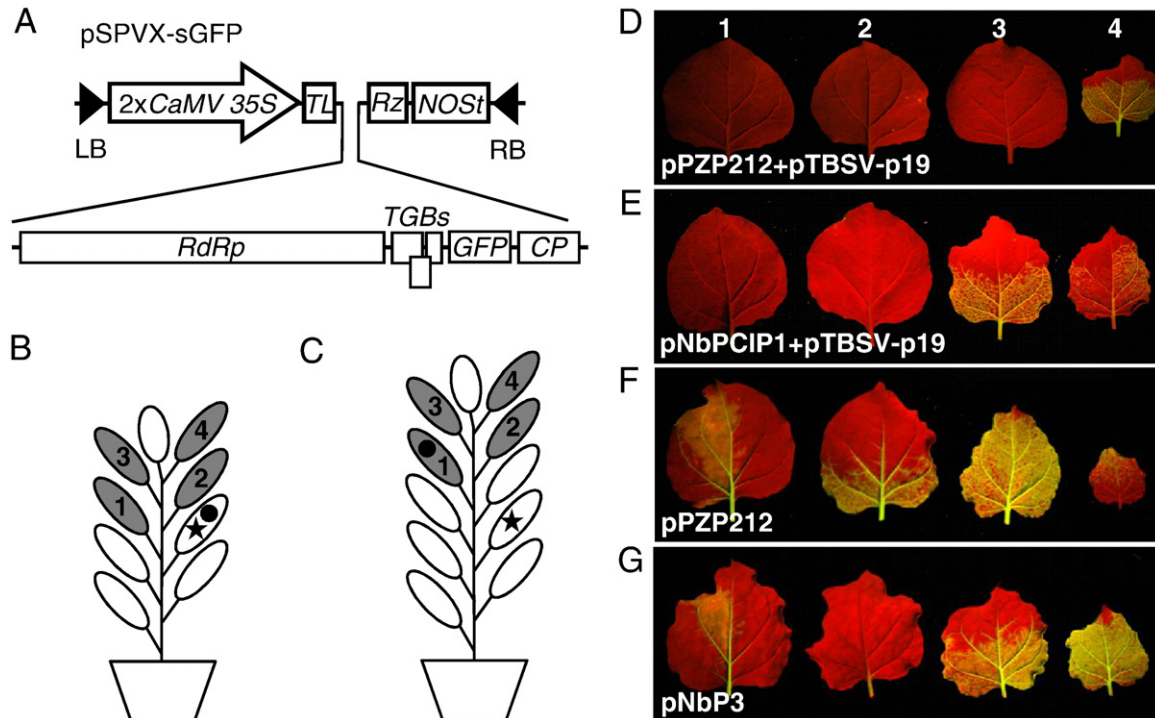
Fig. 11. Effects of NbPCIP1 on viral movement in PVX-infected *N. benthamiana* plants. (A) Schematic representation of sGFP-fused PVX infectious clone (pSPVX-sGFP). pSPVX-sGFP construct was transformed into the *A. tumefaciens* strain GV2260 and agro-infiltrated into *N. benthamiana* plants. (B and C) Schematic representation of NbPCIP1 over-expression and silencing in *N. benthamiana* plants and challenge inoculation with pSPVX-sGFP construct. pPZP212 + pTBSV-p19 and pPZP212 alone infiltrated plants were used as controls for over-expression and silencing experiments, respectively. Closed star represents infiltrated leaves for over-expression or silencing while closed circle represents challenge inoculated leaves with pSPVX-sGFP construct. Leaves observed for GFP fluorescence signal after pSPVX-sGFP inoculation were shaded and numbered. All plants were observed at 5 dpci using the Dark reader™ Hand Lamp HL28T UV Lamp (Clare Chemical Research, Inc., USA).

NbPCIP1 or NbPCIP2 or both are responsible for these phenotypes. Altogether, these results suggest that *NbPCIPs* might be orthologs to these genes. It is not clear, however, how both NbPCIP1 and NbPCIP2 functions in *N. benthamiana* except for the possible role of NbPCIP1 in PVX replication and/or movement and remains further clarification.

As shown in Figs. 9 and 11, we verified that NbPCIP1 interacting with the PVX CP not only positively affects viral RNA accumulation but also viral movement directly and/or indirectly. We speculated that NbPCIPs as well as IP-L, SISENU1, and CaSENU1 orthologs contained ER membrane retention motif (XXRR at the N-terminus or KKXX at the C-terminus)-like KDLE and/or KNLE at the C-terminus (Fig. 1). Interestingly, we observed that the NbPCIP1-sGFP is discretely distributed in granule-like structures throughout the cytoplasm but not in the nucleus (Figs. 6E to H) and found that NbPCIP1-sGFP is mainly associated at ER (Fig. 7C). We also repeatedly observed that the NbPCIP1 in the presence of PVX CP interact with it and co-localized in an inclusion body-like complex in areas surrounding the nucleus (Figs. 8A and B). For most plant viruses, as is stated above, CP plays an essential role in viral movement in host plant (Carrington et al., 1996; Ghoshroy et al., 1997; Lazarowitz and Beachy, 1999). The cell-to-cell movement of PVX requires four virus-encoded proteins, the TGB proteins (25, 12, and 8 kDa proteins) and the CP (Chapman et al., 1992; Fedorkin et al., 2001; Verchot-Lubicz et al., 2007). It has been reported that PVX CP and 25 kDa TGB protein form a complex with viral RNA and this complex require host factor(s) for plasmodesmata trafficking (Lucas, 2006; Morozov and Solovyev, 2003; Verchot-Lubicz, 2005). Recent studies also showed that both 12 and 8 kDa TGB proteins were localized at the ER, ER-associated granular vesicles, and perinuclear X-body and either involved in intracellular transport or interact with the cellular docking sites at the plasmodesmata (Lough et al., 2000; Samuels et al., 2007). These granular vesicles, which align with actin filaments, play an important role in PVX movement (Ju et al., 2005, 2007). In this study, we verified that NbPCIP1 is associated with ER

and when NbPCIP1 interacts with PVX CP, NbPCIP1–PVX CP complex move on areas surrounding nucleus and then formed the inclusion body-like complex such as perinuclear X-body associating PVX TGB proteins (Lough et al., 2000; Samuels et al., 2007). It would be very interesting to know whether the NbPCIP1 localized at the granular vesicles by interacting with PVX CP mediate intracellular transport through an additional interaction with 12 and 8 kDa TGB proteins in ER or ER-associated granular vesicles.

In this regard, it is worth mentioning the recent report showing co-localization of both the IP-L of *N. tabacum* and the majority of ToMV CP in the thylakoid membrane of tobacco chloroplast (Zhang et al., 2008). Since *NbPCIP1* and *IP-L* are ortholog genes as described above, it will be of particular interest to know how proteins of the same gene orthologs localized at different places upon two different virus infections. Since the NbPCIP1 mainly localized in ER or ER-associated granular vesicles upon PVX infection and NbPCIP1–PVX CP interaction as a component in the virus cell-to-cell movement mechanism is still circumstantial, future experiments will involve further characterization of NbPCIP1 localization upon RNA virus infections including potexviruses and determining more detailed functions of virus CP and NbPCIP1 interaction in virus replication and/or cell-to-cell movement mechanism.

Materials and methods

Construction of N. benthamiana cDNA library

N. benthamiana cDNA library was constructed using HybriZAP®-2.1 XR library construction kit and HybridZAP®-2.1 XR cDNA synthesis kit (Stratagene, USA). Poly (A) mRNAs isolated using Oligotex mRNA kit (Qiagen, Germany) from healthy 4-week-old *N. benthamiana* leaves were used for synthesize cDNA. cDNAs were synthesized using oligo (dT) primer and dNTP mixture containing normal dATP, dGTP, dTTP,

and 5-methyl dCTP. Approximately 0.5–2 kb of cDNAs were fractionated using Sepharose CL-2B gel (Stratagene, USA) filtration column and ligated into the HybriZAP®-2.1 vector to generate the primary lambda library. This primary lambda library is amplified, converted by *in vivo* mass excision to a pAD-GAL4-2.1 library as described by the manufacturer's instruction, and used in this work.

N. benthamiana cDNA library screening

The *N. benthamiana* cDNA library was screened using the PVX CP DNA-binding domain fusion pAS2-1 vector (Clontech Laboratories, Inc., USA) as bait. To construct the PVX CP-BD, a PVX CP full-length DNA fragment was prepared by PCR from PVX infectious clone, pSPVX (Park and Kim, 2006), and then cloned into the EcoRI site of pAS2-1 vector. The primer set which was used for this amplification was PVX CP-EcoRI-F and PVX CP-EcoRI-R (Table 3). The PVX CP-BD was transformed into *S. cerevisiae* strain AH109 (MATa, trp1–901, leu2–3, ura3–52, his3–200, galΔ, gal180Δ, LYS2::GAL1$_{UAS}$–GAL1$_{TATA}$–HIS3, GAL2$_{UAS}$–GAL2$_{TATA}$–ADE2, URA3::MEL1$_{UAS}$–MEL1$_{TATA}$–lacZ, MEL1). *N. benthamiana* cDNA library screening was conducted as described by the manufacturer's instruction.

Isolation of NbPCIPs' full-length ORF sequence

To isolate the full-length NbPCIPs' cDNA, total RNAs were isolated from *N. benthamiana* plants and synthesized to cDNA using oligo (dT) 3′ primer (Table 3) by Trizol reagent (Molecular Research Center, Inc., USA). The specific primers, NbPCIP(+2)-EcoRI-F and NbPCIP-EcoRI-R, for full-length NbPCIPs were designed based on the sequences from

the reported full-length ToMV CP interacting protein-L (*IP-L*) cDNA (Li et al., 2005).

Yeast two-hybrid assay

S. cerevisiae strain AH109 were co-transformed with the pACT2 and pAS2-1 fusion derivatives by lithium acetate-mediated yeast transformation method and then selected on synthetic dropout (SD) medium lacking leucine, tryptophan, histidine, and adenine (−LWHA), and leucine and tryptophan (−LW) agar plates. The interactions of SV40 large T antigen$_{(84–708)}$ (pTD1-1) and murine p53$_{(72–390)}$ (pVA3-1) or human lamin C$_{(66–230)}$ (pLAM5′-1) served as positive and negative controls, respectively. Yeast two-hybrid experiments were conducted using the Matchmaker Two-hybrid system 2 based on the yeast two-hybrid system protocols handbook (Clontech Laboratories, Inc., USA).

In vitro protein binding assay

To construct the His-tagged PVX CP and MBP-fused NbPCIP1 for *in vitro* protein binding assay, PVX CP gene and *NbPCIP1* full-length ORF fragment were amplified by PCR from pSPVX (Park and Kim, 2006) and pNbPCIP1-BD and then cloned into the EcoRI site of pET28a(+) vector (EMD chemicals, Inc., Germany) and pMAL-c2X vector (New England Biolabs Inc., USA), respectively. The primer sets which were used for amplification of these fragments were a primer set of PVX CP-EcoRI-F and PVX CP-TAA-EcoRI-R for pET28a(+) cloning and a primer set of NbPCIP1-EcoRI-F and NbPCIP1-EcoRI-R for pMAL-c2X cloning (Table 3). One hundred micrograms of His-tagged PVX CP (PVX CP-

Table 3
Primers used in this study

Primer	Sequence (5′ → 3′)[a]	Application[b]
NbPCIP1 and 2		
NbPCIP(+2)-EcoRI-F	GGAATTCTGGTTCTCCAAACTC	pACT2
NbPCIP-EcoRI-R	GGAATTCTTCCTCCARATCCTTAAGAG	pACT2
NbPCIP-EcoRI-F	GGAATTCGTTCTCCAAACTCAACTTG	pMAL-c2X
NbPCIP1(TAA)-EcoRI-R	GGAATTCTTATTCCTCCAAATCCTTAAGA	pMAL-c2X
NbPCIP-BF	GTTCTCCAAACTCAACTTG	over-expression
NbPCIP1-BR	TTCCTCCAAATCCTTAAGA	BiFC, over-expression
Hisx6 NbPCIP-BF	CATCATCATCATCATCATAGGCCTGTTCTCCAAACTCAACTTG	BiFC
NbPCIP2-BR	TTCCTCCAGATCCTTAAGA	BiFC
NbPCIP1-(199-215)-F	GGCCATGGCGGACACTATG	qRT-PCR
NbPCIP1-(316-297)-R	GTCGACCCCATGCCCATATG	qRT-PCR
NbPCIP1-stop-BR	TTATTCCTCCAAATCCTTAAGA	over-expression
NbP-BF	GGGTCATGGTGGCCA	silencing
PVX CP		
PVX (44-60)-F	GCCCAATTGTTACACACC	qRT-PCR
PVX (161-145)-R	CTATAAGCCTCATCTTG	qRT-PCR
PVX (510-490)-R	GTCTGTTGTGATCTCTGTGAG	RT-PCR
PVX CP-EcoRI-F	GGAATTCTCAGCACCAGCTAGCAC	pAS2-1, pET28a(+)
PVX CP-EcoRI-R	GGAATTCCTCTTTAATTGCTGCTGCCA	pET28a(+)
PVX CP-TAA-EcoRI-R	GGAATTCTTACTCTTTAATTGCTGCTGCCA	pET28a(+)
Hisx6 PVX CP-BF	CATCATCATCATCATCATAGGCCTTCAGCACCAGC TAGCAC	BiFC
PVX CP-BR	TGGTGGTGGGAGA	BiFC, pAS2-1
attB PVX CP-F	GTACAAAAAAGCAGGCTTGTCAGCACCAGCTAGCAC	pSITE-4CA
attB PVX CP-R	GTACAAGAAAGCTGGGTTTGGTGGTGGGAGAGTGC	pSITE-4CA
ubi3-F[c]	GCCGACTACAACATCCAGAAGG	qRT-PCR
ubi3-R[c]	TGCAACACAGCGAGCTTAACC	qRT-PCR
EF1a-F[c]	GATTGGTGGAATTGGTACTACTG	qRT-PCR
EF1a-R[c]	AGCTTCGTGGTGCATCTC	qRT-PCR
Hisx6 ToMV CP-BF	CATCATCATCATCATCATAGGCCTTCTTACGCAATTACTTCTCC	BiFC
ToMV CP-BR	TTAGGATGCAGGTGCA	BiFC
Hisx6 CMV CP-BF	CATCATCATCATCATCATAGGCCTGACAAATCTGAATCAACCAG	BiFC
CMV CP-BR	TCAGACTGGGAGCACTC	BiFC

[a] Restriction enzyme sites (EcoR I) used for cloning were underlined.
[b] pACT2 and pAS2-1 vectors were utilized for yeast-two hybrid assay and pMAL-c2X and ET28a(+) vectors were utilized for *in vitro* binding assay. RFP fusion pSITE-4CA vector was used by gateway technique as described Invitrogen manipulations (Invitrogen, USA).
[c] Primers for ubi3 and EF1a were designed as previously described (Rotenberg et al., 2006).

His) were mixed with 100 μg of MBP-fused NbPCIP1(NbPCIP1-MBP) in binding buffer (20 mM Tris–HCl, pH 7.4, 150 mM NaCl, 1 mM EDTA) and incubated with rotary shaking at 4 °C for 1 h. As a control, the PVX CP-His was incubated with MBP. Bound proteins washed with binding buffer using centrifugation. To these pellets 20 μg of amylase resins and 1 ml of binding buffer were added and incubated with rotary shaking at 4 °C for 2 h and washed five times with binding buffer. Protein pellets were centrifuge at 13,000 rpm for 5 min and resuspended in 2×Laemmli loading buffer (4% SDS, 20% glycerol, 120 mM Tris–HCl, pH6.8, 200 mM DTT, 0.1% bromophenol blue), electrophoresed on 12% SDS polyacrylamide gel, and blotted onto PVDF transfer membranes (Amersham Biosciences, USA; Towbin et al., 1979). The blots were probed with polyclonal antiserum prepared against purified PVX and monoclonal MBP antiserum (New England Biolabs, USA). The products were visualized using a Biotin/StreptA-vidin kit (Amersham Biosciences, USA).

Bimolecular fluorescent complementation (BiFC) assay

For construction of binary plasmids, full-length PVX CP gene, *NbPCIP1* and *NbPCIP2* were amplified by PCR from pPVX CP-BD, pNbPCIP1-AD and pNbPCIP2-AD using specific primers Hisx6 PVX CP-BF and PVX CP-BR for His$_6$ tagged-PVX CP, Hisx6 NbPCIP-BF and NbPCIP1-BR for His$_6$ tagged-NbPCIP1, and Hisx6 NbPCIP-BF and NbPCIP2-BR for His$_6$ tagged-NbPCIP2 (Table 3) and fused as blunt fragments to either the N-terminal portion (1–154 amino acid) of YFPR (NYFP) using StuI site in the binary pPZP212 vector fused to *Tobacco etch virus* (TEV) translational leader (TL) sequence and sGFP (pNbPCIP1-NYFP and pNbPCIP2-NYFP) or to the C-terminal portion (155–238) of YFP (CYFP) in the modified pPZP212 vector (pPVX CP-CYFP) (Morell et al., 2008). As positive and negative controls, pToMV CP-CYFP and pCMV CP-CYFP, respectively, were used for this assay. The full-length ToMV CP and CMV CP genes were amplified by PCR from pToMV CP-BD and pCR3(+) (Seo et al., 2009) using specific primers Hisx6 ToMV CP-BF and ToMV CP-BR for His$_6$ tagged-ToMV CP, Hisx6 CMV CP-BF and CMV CP-BR for His$_6$ tagged-CMV CP (Table 3). The *A. tumefaciens* strain GV2260 were transformed with these constructs and grown on YEP containing selective antibiotics medium for 1 day. Transformed *A. tumefaciens* strain GV2260 harvested by cen-trifugation and suspended in MMA medium (10 mM MES salt (pH 5.6), 10 mM MgCl$_2$ and 200 μM acetosyringone) to an optical density at 600 nm of 0.7, incubated at 30 °C for 2–4 h, and agro-infiltrated in pair-wise combinations together with the p19 silencing suppressor of *Tomato bushy stunt virus* (pTBSV-p19) into *N. benthamiana* leaves using a syringe without a needle. The p19 protein of TBSV was used to suppress gene silencing. Three days after agro-infiltration, agro-infiltrated leaves were observed by epifluorescence microscope (Carl Zeiss, Inc., Germany).

Subcellular localization of NbPCIP1-sGFP and PVX CP-RFP in N. benthamiana protoplasts and epidermal cells

To prepare the sGFP fusion NbPCIP1 (pNbPCIP1-sGFP) and RFP fusion PVX CP (pPVX CP-RFP) construct for co-expression in *N. benthamiana* protoplasts, the *NbPCIP1* full-length ORF fragment was amplified by PCR from pNbPCIP1-BD using specific primers NbPCIP1-BF and NbPCIP1-BR (Table 3). Amplified blunt *NbPCIP1* was cloned into the pPZP212 linearized with StuI site generating pNbPCIP1-sGFP. The PVX CP gene fragment was amplified by PCR from pSPVX clone and then cloned into the pSITE-4CA vector (Chakrabarty et al., 2007) using the Gateway Technology method as described in Invitrogen manipulations (Invitrogen, USA) generating pPVX CP-RFP. The primer set which was used for amplification of PVX CP fragments were attB PVX CP-F and attB PVX CP-R (Table 3). pRFP-ER containing Histidine–Aspartate–Glutamtae–Leucine (HDEL)-ER retention signal-contained marker gene (Chakrabarty et al., 2007) was used as ER marker. All of the resulting constructs are under control of the CaMV 35S promoter

(Fig. 5). The constructs were then introduced into the *A. tumefaciens* strain GV2260 and agro-infiltrated together with the pTBSV p19 into *N. benthamiana* leaves as same with agro-infiltration method for BiFC assay. At 3 days after agro-infiltration, the protoplasts were obtained from agro-infiltrated leaves using enzyme solution (10% mannitol, 0.25 g cellulose, 25 mg macerase, 25 mg BSA). The protoplasts and epidermal cells were observed by epifluorescence microscope (Carl Zeiss, Inc., Germany).

Quantitative real-time RT-PCR analysis

Total RNA was isolated from Mock and PVX-infected *N. benthami-ana* plants by Trizol reagent (Molecular Research Center, Inc., USA) according to manufacturer's instructions and further treated with TURBO DNA-*free*™ (Ambion, USA) to remove genomic DNA. cDNA for detection of *NbPCIP1* mRNA was synthesized from DNase I-treated total RNAs using M-MuLV reverse transcriptase (New England Biolabs, USA) and oligo (dT) 3′ primer. cDNA for detection of PVX RNA was synthesized from DNase I-treated total RNAs using M-MuLV reverse transcriptase (New England Biolabs, USA) and PVX (510–490)-R primer. Quantitative real-time RT-PCR (qRT-PCR) was performed on Applied Biosystems 7500 Fast Real-Time PCR System using the fluorescent SYBR Green method. The qRT-PCR reaction was conducted as described previously using NbPCIP1-(199–215)-F and NbPCIP1-(316–297)-R primer set for detection of NbPCIP1 mRNA and PVX (44–60)-F and PVX (161–145)-R primer set for detection of PVX RNA (Table 3). To normalize the qRT-PCR, two endogenous reference genes, i.e. ubiquitin 3 (*ubi3*) and elongation factor 1α (*EF-1*), were used in each experiment (Rotenberg et al., 2006). Results were expressed as a threshold cycle (C_t) value. Each RNA sample was assayed in triplicate and their C_t values averaged. These averaged values were used in all subsequent calculations. Gene expression was normalized to that of the *ubi3* by subtracting the C_t value of the *ubi3* from the C_t value of the *NbPCIP1* mRNA and PVX RNA to give ΔC_t. Fold induction was calculated by normalizing the data for each time series to that of the 0 hpi sample; the ΔC_t value for that sample was then subtracted from the ΔC_t of the other samples to give a $\Delta\Delta C_t$ value by the Applied Biosystem Detection V 1.3.1 software. Relative expression levels of *NbPCIP1* were compared against the average expression levels of *EF-1*. The $\Delta\Delta C_t$ of NbPCIP1-silencing and over-expression levels were also normalized to *ubi3* and calibrated by mock sample at 11 dpi and 3 dpi, respectively. Lack of variation in PCR products and the absence of primer–dimers were ascertained from the melt curve profile of the PCR products. In all experiments, three biological replicates of each sample type using at least three plants for each time point were tested.

Transient over-expression of NbPCIP1

To prepare the NbPCIP1 without sGFP (NbPCIP1) construct for transient over-expression in *N. benthamiana* plants, the *NbPCIP1* full-length ORF fragment was amplified by PCR from pNbPCIP1-BD using specific primers NbPCIP1-BF and NbPCIP1-BR (Table 3). Amplified blunt NbPCIP1 was cloned into the pPZP212 linearized with StuI and NruI site generating sGFP-deleted pNbPCIP1. The pNbPCIP1 construct was introduced into the *A. tumefaciens* strain GV2260 and agro-infiltrated together with the pTBSV-p19 into *N. benthamiana* leaves as same with agro-infiltration method for BiFC assay. At 3 days after agro-infiltration, the challenge inoculation with purified PVX was carried out in NbPCIP1 over-expressed leaves by mechanical inocula-tion method. The pPZP212 and pTBSV-p19 co-infiltrated *N. benthami-ana* were used as control plants for over-expression experiments.

Transgene silencing of NbPCIP1

To prepare the NbPCIP1 silencing construct, three copies of the partial *NbPCIP1* gene were tandemly fused to the modified pPZP212

vectors (pNbP3 or pNbP3-sGFP). The partial NbPCIP1 fragment (162–465 nt) was amplified by PCR from pNbPCIP1-BD and then cloned into the sGFP-deleted pPZP212 or pPZP212-sGFP vectors using the StuI and NruI site or StuI site, respectively. The specific primer set which was used for amplification of partial *NbPCIP1* fragment were NbP-BF and NbPCIP1-BR (Table 3). The pNbP3 and pNbP3-sGFP constructs were transformed into the *A. tumefaciens* strain GV2260 and agro-infiltrated into *N. benthamiana* leaves as same with agro-infiltration method for BiFC assay. At 11 days after agro-infiltration, the challenge inoculation with purified PVX was carried out in NbPCIP1-silenced upper leaves by mechanical inoculation method. The pPZP212 or pPZP-sGFP infiltrated *N. benthamiana* were used as control plants for silencing experiments.

Detection of PVX movement in N. benthamiana plants

To carry out viral movement experiment, sGFP was fused to pSPVX (Park and Kim, 2006) clone (pSPVX-sGFP, Fig. 11A). NbPCIP1 was over-expressed and silenced in *N. benthamiana* leaves using pNbPCIP1 and pNbP3 constructs, respectively (Fig. 5). *A. tumefaciens* strain GV2260 transformed with pPZP212, pNbPCIP1 or pNbP3 constructs were infiltrated (optical density of 0.7 at 600 nm) into *N. benthamiana* leaves. pPZP212 construct was used as control and pTBSV-p19 construct was co-infiltrated for over-expression experiment. The pNbPCIP1 and pNbP constructs transformed into the *A. tumefaciens* strain GV2260 were agro-infiltrated together with the pTBSV-p19 and alone into *N. benthamiana* leaves, respectively, as same with agro-infiltration method for BiFC assay. At 3 days and 11 days after agro-infiltration, the pSPVX-sGPF-transformed *A. tumefaciens* strain GV2260 were agro-infiltration in NbPCIP1 over-expressed leaves or in NbPCIP1 silenced upper leaves and than were observed for GFP expression for 5 days under the Dark reader™ Hand Lamp HL28T UV Lamp (Clare Chemical Research, Inc., USA).

Computer-aided analysis of subcellular localization

The motif of amino acid sequences for subcellular localization signals were predicted using the PSORT software (http://123geno-mics.com, Nakai and Horton, 2007).

Statistical analysis

Data were statistically analyzed by analysis of variance (ANOVA) and means were compared using the Fisher's LSD (Least significant difference) test. Statistical analysis was performed with SAS (version 9.1; SAS Institute Inc., USA).

Acknowledgments

References

Agros, P., Tsukihara, T., Rossmann, M.G., 1980. A structural comparison of concanavalin A and tomato bushy stunt virus protein. J. Mol. Evol. 15, 169–179.

Bercks, R., 1970. *Potato virus X*. CMI/AAB descriptions of plant viruses. Commomwealth, Kew, England no. 111.

Callaway, A., Giesman-Cookmeyer, D., Gillock, E.T., Sit, T.L., Lommel, S.A., 2001. The multifunctional capsid proteins of plant RNA viruses. Annu. Rev. Phytopathol. 39, 419–460.

Carrington, J.C., Kasschau, K.D., Mahajan, S.K., Schaad, M.C., 1996. Cell-to-cell and long-distance transport of viruses in plants. Plant Cell 8, 1669–1681.

Chakrabarty, R., Banerjee, R., Chung, S.M., Farman, M., Citovsky, V., Hogenhout, S.A., Tzfira, T., Goodin, M., 2007. pSITE vectors for stable integration or transient expression of autofluorescent protein fusions in plants: probing *Nicotiana benthamiana*-virus interactions. Mol. Plant-Microb. Interact. 20, 740–750.

Chapman, S., Kavanagh, T., Baulcombe, D., 1992. *Potato virus X* as a vector for gene expression in plants. Plant J. 2, 549–557.

Chen, Z., Zhou, T., Wu, X., Hong, Y., Fan, Z., Li, H., 2008. Influence of cytoplasmic heat shock protein 70 on viral infection of *Nicotiana benthamiana*. Mol. Plant Pathol. 9, 809–817.

Diez, J., Ishikawa, M., Kaido, M., Ahlquist, P., 2000. Identification and characterization of a host protein required for efficient template selection in viral RNA replication. Proc. Natl. Acad. Sci. U.S.A. 97, 3913–3918.

Fedorkin, O., Solovyev, A., Yelina, N., Zamyatnin Jr., A., Zinovkin, R., Makinen, K., Schiemann, J., Yu Morozov, S., 2001. Cell-to-cell movement of *Potato virus X* involves distinct functions of the coat protein. J. Gen. Virol. 82, 449–458.

Gamarnik, A.V., Andino, R., 1998. Switch from translation to RNA replication in a positive-stranded RNA virus. Genes Dev. 12, 2293–2304.

Ghoshroy, S., Lartey, R., Sheng, J., Citovsky, V., 1997. Transport of proteins and nucleic acids through plasmodesmata. Annu. Rev. Plant Physiol. Plant Mol. Biol. 48, 27–50.

Goodin, M.M., Zaitlin, D., Naidu, R.A., Lommel, S.A., 2008. *Nicotiana benthamiana*: its history and future as a model for plant–pathogen interactions. Mol. Plant-Microb. Interact. 21, 1015–1026.

Hofius, D., Maier, A.T., Dietrich, C., Jungkunz, I., Bornke, F., Maiss, E., Sonnewald, U., 2007. Capsid protein-mediated recruitment of host *DnaJ*-like proteins is required for *Potato virus Y* infection in tobacco plants. J. Virol. 81, 11870–11880.

Hu, B., Pillai, N., Hemenway, C., 2007. Long-distance RNA–RNA interactions between terminal elements and the same subset of internal elements on the *Potato virus X* genome mediate minus- and plus-strand RNA synthesis. RNA 13, 267–280.

Huisman, M.J., Linthorst, H.J., Bol, J.F., Cornelissen, J.C., 1988. The complete nucleotide sequence of *Potato virus X* and its homologies at the amino acid level with various plus-stranded RNA viruses. J. Gen. Virol. 69, 1789–1798.

Ishikawa, M., Diez, J., Restrepo-Hartwig, M., Ahlquist, P., 1997. Yeast mutations in multiple complementation groups inhibit *Brome mosaic virus* RNA replication and transcription and perturb regulated expression of the viral polymerase-like gene. Proc. Natl. Acad. Sci. U.S.A. 94, 13810–13815.

John, I., Hackett, R., Cooper, W., Drake, R., Farrell, A., Grierson, D., 1997. Cloning and characterization of tomato leaf senescence-related cDNAs. Plant Mol. Biol. 33, 641–651.

Ju, H.J., Samuels, T.D., Wang, Y.S., Blancaflor, E., Payton, M., Mitra, R., Krishnamurthy, K., Nelson, R.S., Verchot-Lubicz, J., 2005. The *Potato virus X* TGBp2 movement protein associates with endoplasmic reticulum-derived vesicles during virus infection. Plant Physiol. 138, 1877–1895.

Ju, H.J., Brown, J.E., Ye, C.M., Verchot-Lubicz, J., 2007. Mutations in the central domain of *Potato virus X* TGBp2 eliminate granular vesicles and virus cell-to-cell trafficking. J. Virol. 81, 1899–1911.

Karpova, O.V., Arkhipenko, M.V., Zaiakina, O.V., Nikitin, N.A., Kiseleva, O.I., Kozlovskii, S.V., Rodionova, N.P., Atabekov, I.G., 2006. [Translational regulation of *Potato virus X* RNA-coat protein complexes: the key role of a coat protein N-terminal peptide]. Mol. Biol. (Mosk.) 40, 703–710.

Kim, K.-H., Hemenway, C.L., 1996. The 5′ nontranslated region of *Potato virus X* RNA affects both genomic and subgenomic RNA synthesis. J. Virol. 70, 5533–5540.

Kim, K.-H., Kwon, S.-J., Hemenway, C.L., 2002. Cellular protein binds to sequences near the 5′ terminus of *Potato virus X* RNA that are important for virus replication. Virology 301, 305–312.

Krab, I.M., Caldwell, C., Gallie, D.R., Bol, J.F., 2005. Coat protein enhances translational efficiency of *Alfalfa mosaic virus* RNAs and interacts with the eIF4G component of initiation factor eIF4F. J. Gen. Virol. 86, 1841–1849.

Kwon, S.-J., Park, M.-R., Kim, K.-W., Plante, C.A., Hemenway, C.L., Kim, K.-H., 2005. *cis*-Acting sequences required for coat protein binding and in vitro assembly of *Potato virus X*. Virology 334, 83–97.

Lazarowitz, S.G., Beachy, R.N., 1999. Viral movement proteins as probes for intracellular and intercellular trafficking in plants. Plant Cell 11, 535–548.

Li, Y., Wu, M.Y., Song, H.H., Hu, X., Qiu, B.S., 2005. Identification of a tobacco protein interacting with *Tomato mosaic virus* coat protein and facilitating long-distance movement of virus. Arch. Virol. 150, 1993–2008.

Lough, T.J., Netzler, N.E., Emerson, S.J., Sutherland, P., Carr, F., Beck, D.L., Lucas, W.J., Forster, R.L., 2000. Cell-to-cell movement of potexviruses: evidence for a ribonucleoprotein complex involving the coat protein and first triple gene block protein. Mol. Plant-Microb. Interact. 13, 962–974.

Lough, T.J., Lee, R.H., Emerson, S.J., Forster, R.L., Lucas, W.J., 2006. Functional analysis of the 5′ untranslated region of potexvirus RNA reveals a role in viral replication and cell-to-cell movement. Virology 351, 455–465.

Lu, B., Stubbs, G., Culver, J.N., 1998. Coat protein interactions involved in *Tobacco mosaic tobamovirus* cross-protection. Virology 248, 188–198.

Lucas, W.J., 2006. Plant viral movement proteins: agents for cell-to-cell trafficking of viral genomes. Virology 344, 169–184.

Ma, C., Mitra, A., 2002. Intrinsic direct repeats generate consistent post-transcriptional gene silencing in tobacco. Plant J. 31, 37–49.

Miller, E.D., Plante, C.A., Kim, K.-H., Brown, J.W., Hemenway, C.L., 1998. Stem–loop structure in the 5′ region of *Potato virus X* genome required for plus-strand RNA accumulation. J. Mol. Biol. 284, 591–608.

Miller, E.D., Kim, K.-H., Hemenway, C.L., 1999. Restoration of a stem–loop structure required for *Potato virus X* RNA accumulation indicates selection for a mismatch and a GNRA tetraloop. Virology 260, 342–353.

Morell, M., Espargaro, A., Aviles, F.X., Ventura, S., 2008. Study and selection of *in vivo* protein interactions by coupling bimolecular fluorescence complementation and flow cytometry. Nat. Protoc. 3, 22–33.

Morozov, S.Y., Solovyev, A.G., 2003. Triple gene block: modular design of a multifunctional machine for plant virus movement. J. Gen. Virol. 84, 1351–1366.

Nakai, K., Horton, P., 2007. Computational prediction of subcellular localization. Methods Mol. Biol. 390, 429–466.

Okinaka, Y., Mise, K., Okuno, T., Furusawa, I., 2003. Characterization of a novel barley protein, HCP1, that interacts with the *Brome mosaic virus* coat protein. Mol. Plant-Microb. Interact. 16, 352–359.

Oparka, K.J., Roberts, A.G., Roberts, I.M., Prior, D.A.M., Crus, S.S., 1996. Viral coat protein is targeted to, but does not gate, plasmodesmata during cell-to-cell movement of *Potato virus X*. Plant J. 10, 805–813.

Park, S.-H., Kim, K.-H., 2006. Agroinfiltration-based *Potato virus X* replications to dissect the requirements of viral Infection. Plant Pathol. J. 22, 386–390.

Park, M.-R., Kwon, S.-J., Choi, H.S., Hemenway, C.L., Kim, K.-H., 2008a. Mutations that alter a repeated ACCA element located at the 5′ end of the *Potato virus X* genome affect RNA accumulation. Virology 378, 133–141.

Park, M.-R., Park, S.-H., Cho, S.-Y., Hemenway, C.L., Choi, H.S., Sohn, S.H., Kim, K.-H., 2008b. RNA-RNA interactions between RNA elements at the 5′ end at the upstream of sgRNA of RNA genome are required for *Potato virus X* RNA replication. Plant Pathol. J. 24, 289–295.

Pillai-Nair, N., Kim, K.-H., Hemenway, C.L., 2003. *Cis*-acting regulatory elements in the *Potato virus X* 3′ non-translated region differentially affect minus-strand and plus-strand RNA accumulation. J. Mol. Biol. 326, 701–720.

Rotenberg, D., Thompson, T.S., German, T.L., Willis, D.K., 2006. Methods for effective real-time RT-PCR analysis of virus-induced gene silencing. J. Virol. Methods 138, 49–59.

Samuels, T.D., Ju, H.J., Ye, C.M., Motes, C.M., Blancaflor, E.B., Verchot-Lubicz, J., 2007. Subcellular targeting and interactions among the *Potato virus X* TGB proteins. Virology 367, 375–389.

Skryabin, K.G., Morozov, S., Kraev, A.S., Rozanov, M.N., Chernov, B.K., Lukasheva, L.I., Atabekov, J.G., 1988. Conserved and variable elements in RNA genomes of potexviruses. FEBS Lett. 240, 33–40.

Seo, J.-K., Kwon, S.-J., Choi, H.-S., Kim, K.-H., 2009. Evidence for alternate states of *Cucumber mosaic virus* replicase assembly in positive- and negative-strand RNA synthesis. Virology 383, 248–260.

Strauss, J.H., Strauss, E.G., 1999. Viral RNA replication. With a little help from the host. Science 283, 802–804.

Towbin, H., Staehelin, T., Gordon, J., 1979. Electrophoretic transfer of proteins from polyacrylamide gels to nitrocellulose sheets: procedure and some applications. Proc. Natl. Acad. Sci. U.S.A. 76, 4350–4353.

Verchot-Lubicz, J., 2005. A new cell-to-cell transport model for potexviruses. Mol. Plant-Microb. Interact. 18, 283–290.

Verchot-Lubicz, J., Ye, C.M., Bamunusinghe, D., 2007. Molecular biology of potexviruses: recent advances. J. Gen. Virol. 88, 1643–1655.

Zhang, C., Liu, Y., Sun, X., Qian, W., Zhang, D., Qiu, B., 2008. Characterization of a specific interaction between IP-L, a tobacco protein localized in the thylakoid membranes, and *Tomato mosaic virus* coat protein. Biochem. Biophys. Res. Commun. 374, 253–257.